



# Aerodynamic interference effects between a triple-box girder and trains on aerodynamic forces and vortex-induced vibration

YANG Ling-bo(杨凌波)<sup>1</sup>, HUA Xu-gang(华旭刚)<sup>1</sup>, WANG Chao-qun(王超群)<sup>1\*</sup>,  
HE Dong-sheng(何东升)<sup>2</sup>, CHEN Zheng-qing(陈政清)<sup>1</sup>

1. Key Laboratory for Wind and Bridge Engineering of Hunan Province, Hunan University, Changsha 410082, China;
2. China Railway Major Bridge Reconnaissance & Design Institute Co., Ltd., Wuhan 430050, China

© Central South University 2022

**Abstract:** Wind tunnel tests were carried out to investigate the aerodynamic interference between a triple-box girder and trains, involving static aerodynamic forces and vortex-induced vibrations (VIVs). Static and dynamic sectional models of the girder and trains were employed for aerodynamic force measurement and VIV test, respectively. Results indicate that the aerodynamic interference effect on static aerodynamic forces of both the girder and trains is remarkable. When a single train exists, the horizontal position of the train has a small effect on aerodynamic coefficients of the girder. When two trains meet on the girder, the drag coefficient of the girder is significantly reduced compared with that of without train or with a single train; besides, during the whole meeting process, aerodynamic forces of the leeward train first drop and then increase suddenly. The fluctuation of aerodynamic force could cause redundant vibration of the train, which is unfavorable for safety and comfort. A train on the girder could worsen the girder VIV performance: a new vertical VIV appears in the triple-box girder when a train is on the girder, and the torsional VIV amplitude increases significantly when the train is on the windward side.

**Key words:** triple-box girder; wind tunnel test; train-girder system; aerodynamic interference; vortex-induced vibration

**Cite this article as:** YANG Ling-bo, HUA Xu-gang, WANG Chao-qun, HE Dong-sheng, CHEN Zheng-qing. Aerodynamic interference effects between a triple-box girder and trains on aerodynamic forces and vortex-induced vibration [J]. Journal of Central South University, 2022, 29(8): 2532–2541. DOI: <https://doi.org/10.1007/s11771-022-5104-8>.

## 1 Introduction

In research on wind resistance of a rail-cum-road bridge, aerodynamic coefficients and vortex-induced vibration (VIV) are focused. The static wind load acting on train-girder system directly affects the comfort and safety of the train [1–2]; therefore, it is necessary to study the variation law of aerodynamic coefficients of the train-girder

system in wind resistant design of bridges [3–6]. Besides, there is a possibility for the train to stay on the bridge for a long time due to some emergency circumstances, such as communication failure, mechanical failure and power failure. This kind of emergency is infrequent in general, but once it occurs, the train might change the VIV performance of the girder for which the consequences might be very serious. In view of this, it is necessary to study the influence of the train on VIV performance of the

**Foundation item:** Project(52025082) supported by the National Natural Science Foundation for Distinguished Young Scholars of China; Project(CX20190288) supported by Hunan Provincial Innovation Foundation for Postgraduate, China

**Received date:** 2021-06-22; **Accepted date:** 2021-12-05

**Corresponding author:** WANG Chao-qun, PhD candidate; E-mail: [cqwang@hnu.edu.cn](mailto:cqwang@hnu.edu.cn); ORCID: <https://orcid.org/0000-0002-2127-4110>

girder. Due to its excellent aeroelastic stability and traffic capacity, triple-box girder is becoming a recommendable structural style for a super-long span rail-cum-road bridge [7]. However, there are few reports on its aerodynamic characteristics at present.

In recent decades, a large number of scholars have studied the aerodynamic interference between trains and girder which affects the aerodynamic characteristics of the train and system (e. g., the aerodynamic forces acting on the train and the bridges) [8]. Under the action of crosswind, the geometry of the girder section will affect the aerodynamic force of the train when the train passes by the bridge [9]. In addition, the presence of the train will also change the flow field structure of the girder and the aerodynamic force acting on the girder. Aerodynamic forces and aerodynamic parameters of the train and the girder are usually obtained by wind tunnel test and computational fluid dynamics (CFD) numerical simulation [10 – 11]. The dramatic fluctuation of the wind load acting on the train due to the aerodynamic interference between the train and the girder might cause supernumerary vibration, which is unfavorable for the safety and comfort of the train [12–14].

VIV performance of the girder is extremely significant for the wind resistance design of bridge. Previous studies have found that some auxiliary facilities have a great impact on the VIV performance of the girder. Therefore, it is a common research method to improve the VIV performance of the girder by adjusting the auxiliary facilities. LARSEN et al [15] conducted sectional model wind tunnel test of Stonecutters bridge with different scale ratios, and found that the deflector can improve the VIV performance of the girder at high Reynolds number. Many factors also affect the VIV performance of the girder [16 – 17]. For example, with the increase of structural damping ratio, the VIV amplitude gradually decreased, and the “lock-in” region gradually narrowed [18]. Under the action of crosswind, the flow field structure around the triple-box girder is extraordinary complex, and its mechanism needs to be explored by CFD and flow visualization technology. At present, few scholars have studied the effect of aerodynamic interference between train and girder on VIV

performance of the girder.

Due to the lack of engineering practice, there are few studies on the aerodynamic characteristics of the train-girder system of the triple-box girder. Messina bridge (with a main span of 3300 m) in Italy is the first bridge to adopt the triple-box girder scheme in design stage although it is not practiced. In the design process of the bridge, DIANA et al carried out a series of experimental studies on aerodynamic performance of streamlined triple-box girder [19 – 20]. Taoyaomen rail-cum-road bridge (cable-stayed bridge, main span: 666 m) and Xihoumen rail-cum-road bridge (cable-stayed-suspension system, main span: 1488 m) under construction are the first bridges adopting triple-box girder for engineering practice in the world. The triple-box girder is adopted for the Xihoumen rail-cum-road bridge to avoid flutter instability. Additionally, the two bridges are closely connected by Cezi Isle with a small distance of about 2 km; hence a similar triple-box girder was also adopted for Taoyaomen bridge to ensure the continuity of the high-speed railway line and highway alignment, although the main span of it is rather short. Due to the complexity of the cross-section structure of the triple-box girder, it can be inferred that the flow field characteristics of the triple-box girder may be more complex than that of the ordinary streamline section or even the twin-box girder [21].

In this paper, a series of wind tunnel tests are carried out to investigate the aerodynamic interference between trains and the triple-box girder of bridges. Static and dynamic sectional models of the trains and the girder are employed for aerodynamic force measurement and VIV test, respectively. Based on the test results, the aerodynamic interference effect on aerodynamic forces of the train-girder system as well as the VIV performance of the girder is analyzed and discussed.

## 2 Outline of wind tunnel tests

### 2.1 Experimental setup

The wind tunnel test is carried out in HD-2 boundary layer wind tunnel of Key Laboratory for Wind and Bridge Engineering of Hunan province, China. The test section is 3 m in width and 2.5 m in height and the incoming flow from the test section is uniform flow. The turbulent intensity is less than

0.5% when the wind speed is more than 3 m/s.

In the design stage of Taoyaomen Rail-cum-Road Bridge, there are several alternative cross sections with different web shapes for the triple-box girder [21], and only limited tests have been carried out on each section during the design stage due to the heavy workload. Figure 1 depicts two cross sections with linear-type webs which showed relatively good VIV performance. Except for the difference of web shape, other geometric characteristics of the two sections are almost the same; hence the aerodynamic characteristics of the two cross sections are similar [21] both in aerodynamic coefficients and VIV performance. In view of this, as a case study, the authors only present the limited results in this paper. Without loss of generality, Section I is adopted for force measurement test and Section II for VIV test. The girder has a constant height of  $H=4.5$  m, while the width of cross sections I and II are 65.6 m and 66 m, respectively. Specifically, the width of railway girder is 13 m, and the width of each highway girder is 19 m.

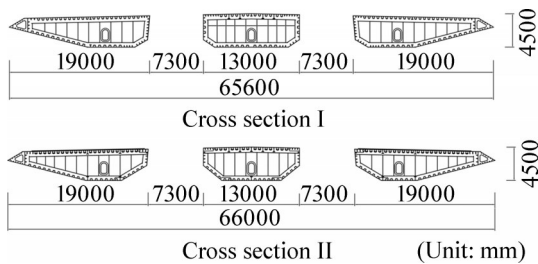


**Figure 1** Cross sections of the bare girder with different web shapes

The scaling factor  $\lambda_s$  of the sectional models of the girder and trains are 1:60, and the total length of them is 2.4 m. The prototype of the train is China Railway High-speed 3 (CRH3) with section width  $b=0.0544$  m and height  $h=0.0604$  m (excluding wheel height). Detailed geometric parameters of the test models are listed in Table 1. Dynamic parameters of the bridge in Table 1 are obtained through three-dimensional finite element modelling, which is widely used for the replacement of field measurement [22].

**2.2 Aerodynamic force measurement**

As a bridge carries double-track railway, there are a number of combinations of the train and the

**Table 1** Parameters of the sectional model

Object	Parameter	Prototype	Sectional model
Bridge	Geometry scale ratio, $\lambda_s$		1/60
	Height, $H$ / m	4.5	0.075
	Width, $B$ / m	65.6, 66.0	1.1
	Length, $L$ / m	666.0	2.4
	Mass per meter, $m$ /( $\text{kg}\cdot\text{m}^{-1}$ )	63617	17.67
	Inertial moment per meter, $I$ /( $\text{kg}\cdot\text{m}^2\cdot\text{m}^{-1}$ )	$2.01\times 10^7$	1.55
	Vertical natural frequency, $f_v$ /Hz	0.286	3.418
	Torsional natural frequency, $f_a$ /Hz	0.438	5.371
	Vertical damping ratio, $\zeta_v$ /%	0.31	0.30
	Torsional damping ratio, $\zeta_a$ /%	0.30	0.33
Train	Height, $h$ /m	3.624	0.0604
	Width, $b$ /m	3.264	0.0544
	Length, $l$ /m	—	2.4
	Mass per meter, $m_t$ /( $\text{kg}\cdot\text{m}^{-1}$ )	105	1.75

girder conditions. Table 2 shows the test cases of aerodynamic interference force measurement of the train-girder system. Limited by the experimental setup, slight but macroscopic VIV will occur at a lower wind speed range (5 – 8 m/s) for the rigid mounted sectional model, which could lead to unacceptable test error of the force measurement. On the other hand, an overlarge wind speed could lead to excessive aerodynamic forces acting on the sectional model which might damage the balances. In view of this, the applicable wind speed range of 10–20 m/s (10, 15 and 20 m/s) is selected for the force measurement.

**Table 2** Aerodynamic force measurement test case of the girder-train system (Section I)

Test case	Test object	System state description
A1	Girder only	Girder model
A2	Girder and windward train	Train track 1
A3	Girder and leeward train	Train track 2
A4	Girder, windward side train and leeward side train	Train track 1 and Train track 2

Section I in completed state with aerodynamic measures for VIV mitigation is adopted for force measurement. The main aerodynamic measures [23] consist of: replacing the original stripe-type wind

barrier of highway girder (with a total height of 3 m) by a grid-type wind barrier (with a total height of 4 m); moving the two maintenance tracks under the highway girder to the position directly below the inner web; blocking the half part of the crash barrier (at the middle height of the barrier height); using 35% porous grid plates to seal the girder slots.

The aerodynamic force measuring system consists of two six-component balances and an ultrasonic anemometer. During the test, the model is horizontally installed on six-component balance through a specially designed support (Figure 3). The time history of aerodynamic force acting on the model under a specific wind speed and wind attack angle is directly measured. The average value of time history of aerodynamic force is calculated to obtain the dimensionless aerodynamic coefficients under the wind attack angle. During the test, the aerodynamic force measurement of the girder and two trains is realized by changing the positions of the two six-component balances at both ends of the model. The six-component balances at three different installation positions are shown in Figure 3. Figure 4 shows the installation diagram of sectional models in wind tunnel for force measurement.

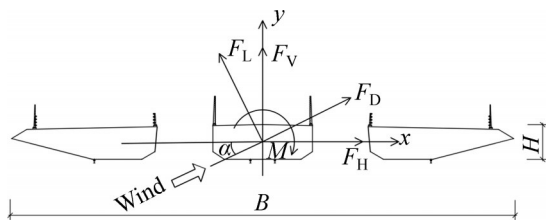


**Figure 2** Aerodynamic forces on completed triple-box girder

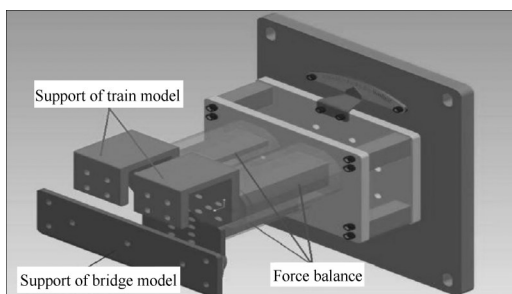


**Figure 3** Aerodynamic force measurement support

**2.3 Vortex-induced vibration test**

As mentioned in the introduction, there is a possibility for the train to stay on the bridge for a long time due to some emergency circumstances.

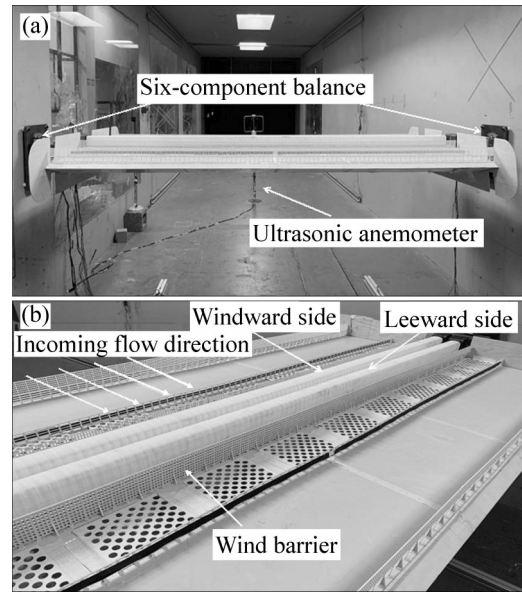


**Figure 4** Installation diagram of force measurement test: (a) Balance installation diagram; (b) Train installation diagram

Once this kind of emergency occurs, the train might change the VIV performance of the bridge girder. In view of this, it is necessary to study the influence of the train on the VIV performance of the girder.

Sectional model of the girder with Section II is employed for the VIV test. Cases for VIV test are shown in Table 3. The wind speed range of wind tunnel in VIV test is 0–10.2 m/s. The influence of the train on VIV performance of the girder is studied at  $\alpha=0^\circ$ .

**Table 3** VIV test case of the girder-train system (Section II )

Test case	Test object	System state description
B1	Girder only	Girder model
B2	Girder and windward train	Train track 1
B3	Girder and leeward train	Train track 2

In fact, the train is not very long and shorter than the girder, which could cause a three-dimensional aerodynamic interference (which is affected by the length, spanwise position, as well as the end effects of the train) on the bridge girder. However, as a preliminary study, this paper is only focused on the aerodynamic performance of the two-dimensional cross section of the train-girder system by employing sectional models, and the three-

dimensional effect caused by the limit length of train is not considered in this paper.

The VIV test system consists of four laser displacement sensors and ultrasonic anemometer. In order to avoid local deformation caused by insufficient stiffness of the girder model, four laser displacement sensors were arranged at  $L/2$  and  $L/4$  of the model respectively to collect displacement response at  $L/2$  and  $L/4$  of the sectional model during the test. The installation of aerodynamic force measurement model is shown in Figure 5.

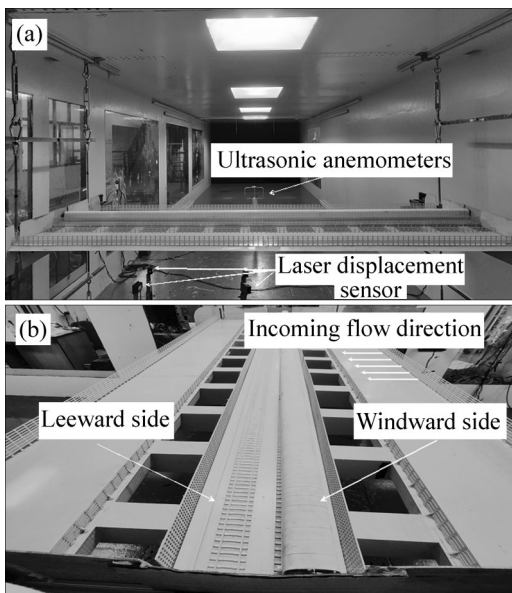


**Figure 5** Installation diagram of VIV test: (a) Laser displacement sensor installation diagram; (b) Train installation diagram

### 3 Results of aerodynamic force measurement

#### 3.1 Aerodynamic coefficient

Definitions of aerodynamic forces for the girder and train are shown in Figure 2 and Figure 6, respectively. It should be noted that the moment center of the train is defined at the center of the top of the two train tracks (i.e., the bottom of the train wheel). Aerodynamic coefficients of the girder in wind axis coordinate system are defined as follows:

$$C_D(\alpha) = \frac{F_D}{0.5\rho U^2 HL} \quad (1)$$

$$C_L(\alpha) = \frac{F_L}{0.5\rho U^2 BL} \quad (2)$$

$$C_M(\alpha) = \frac{M}{0.5\rho U^2 B^2 L} \quad (3)$$

where  $C_D(\alpha)$ ,  $C_L(\alpha)$  and  $C_M(\alpha)$  denote the drag, lift

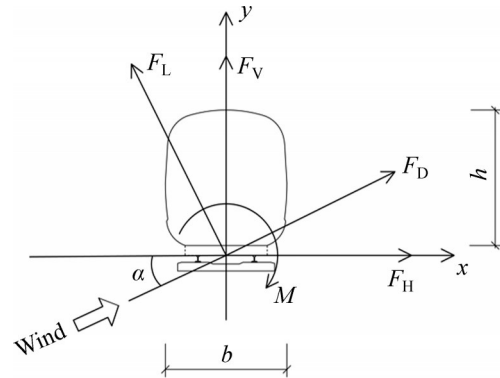


**Figure 6** Aerodynamic forces on the train

and moment coefficients in wind axis coordinate system respectively;  $\alpha$  is the wind attack angle;  $U$  is the test wind speed;  $\rho=1.225 \text{ kg/m}^3$  denotes the air density. For comparison convenience, the width and height of bare girder (i.e.,  $B=1.093 \text{ m}$  and  $H=0.075 \text{ m}$ ) are adopted when calculating the aerodynamic coefficients of the girder in this study.

#### 3.2 Reynolds number effect

For a bluff body, the separation point of uniform flow could be affected by the Reynolds number [24]; hence the aerodynamic performance could be related to the Reynolds number effect. In view of this, wind tunnel test of aerodynamic force measurement for the train-girder system (case A2) is carried out at  $U=10 \text{ m/s}$ ,  $15 \text{ m/s}$  and  $20 \text{ m/s}$  respectively at  $\alpha=0^\circ$ .

Aerodynamic coefficients  $C_H(\alpha)$  and  $C_V(\alpha)$  of the train-girder system in body axis coordinate system are obtained as shown in Table 4. It is apparent that the aerodynamic coefficients of the train-girder system vary slightly under different wind speeds. In other words, the effect of Reynolds number is very small and could be ignored. Therefore, the results given in Tables 5–7 are the average values of the aerodynamic coefficients for all test wind speeds.

#### 3.3 Aerodynamic interference effect on aerodynamic forces

##### 3.3.1 Train-girder system with single train

Table 5 shows the aerodynamic coefficients of bridge without train at  $\alpha=0^\circ$ . It should be noted that the aerodynamic coefficients of the train model in Table 5 are obtained from the CRH2 train [25], of which the cross-section shape is very similar to the

**Table 4** Aerodynamic coefficients of the girder and train under different wind speeds

Wind speed/ (m·s <sup>-1</sup> )	Aerodynamic coefficients of train			Aerodynamic coefficients of girder		
	C <sub>H</sub>	C <sub>V</sub>	C <sub>M</sub>	C <sub>H</sub>	C <sub>V</sub>	C <sub>M</sub>
10	0.096	0.126	0.085	1.457	-0.200	-0.013
15	0.099	0.139	0.078	1.472	-0.205	-0.013
20	0.110	0.152	0.079	1.468	-0.217	-0.008
Mean value	0.101	0.139	0.081	1.465	-0.207	-0.011

**Table 5** Aerodynamic coefficients of a single train or girder at  $\alpha=0^\circ$

Test case	Test object	C <sub>H</sub>	C <sub>V</sub>	C <sub>M</sub>
Reference case	Train model [25]	1.613	—	—
A1	Girder model	1.633	-0.174	-0.007

**Table 6** Aerodynamic coefficients of the train-girder system (single train) at  $\alpha=0^\circ$

Test case	Track	Aerodynamic coefficients of train			Aerodynamic coefficients of girder		
		C <sub>H</sub>	C <sub>V</sub>	C <sub>M</sub>	C <sub>H</sub>	C <sub>V</sub>	C <sub>M</sub>
A2	1	0.101	0.139	0.081	1.465	-0.207	-0.011
A3	2	0.097	0.142	0.074	1.470	-0.218	-0.012

**Table 7** Aerodynamic coefficients of the train-girder system (double trains)

Test case	Track	Aerodynamic coefficients of train			Aerodynamic coefficients of girder		
		C <sub>H</sub>	C <sub>V</sub>	C <sub>M</sub>	C <sub>H</sub>	C <sub>V</sub>	C <sub>M</sub>
A4	1	0.113	0.171	0.083	1.158	-0.207	-0.012
	2	0.024	0.043	0.015			

CRH3 train in this study. In fact, the difference of drag coefficient between CRH2 and CRH3 train measured at low wind speed is very small and could be ignored [26].

In order to study the aerodynamic interaction between the girder and the train when a single train is at different positions on the girder, the aerodynamic coefficients of the train and the girder at  $\alpha=0^\circ$  are obtained as shown in Table 6.

According to Table 6, when the train stays on the girder, the drag coefficient of the train decreases significantly due to the blocking effect of the wind barrier, and the drag coefficient of the girder decreases slightly due to the existence of the train. The horizontal position of the train (i. e., on train track 1 or train track 2) has little effects on the

aerodynamic coefficients of both the train and the girder. The existence of the train slightly increases the lift coefficient of the girder, while it has little influence on the moment coefficient of the girder.

### 3.3.2 Train-girder system with double trains

Since the girder is used for a double-track railway bridge, the two trains may meet on the girder. Aerodynamic coefficients of trains and the girder are shown in Table 7 when double trains exist simultaneously on the girder at  $\alpha=0^\circ$ .

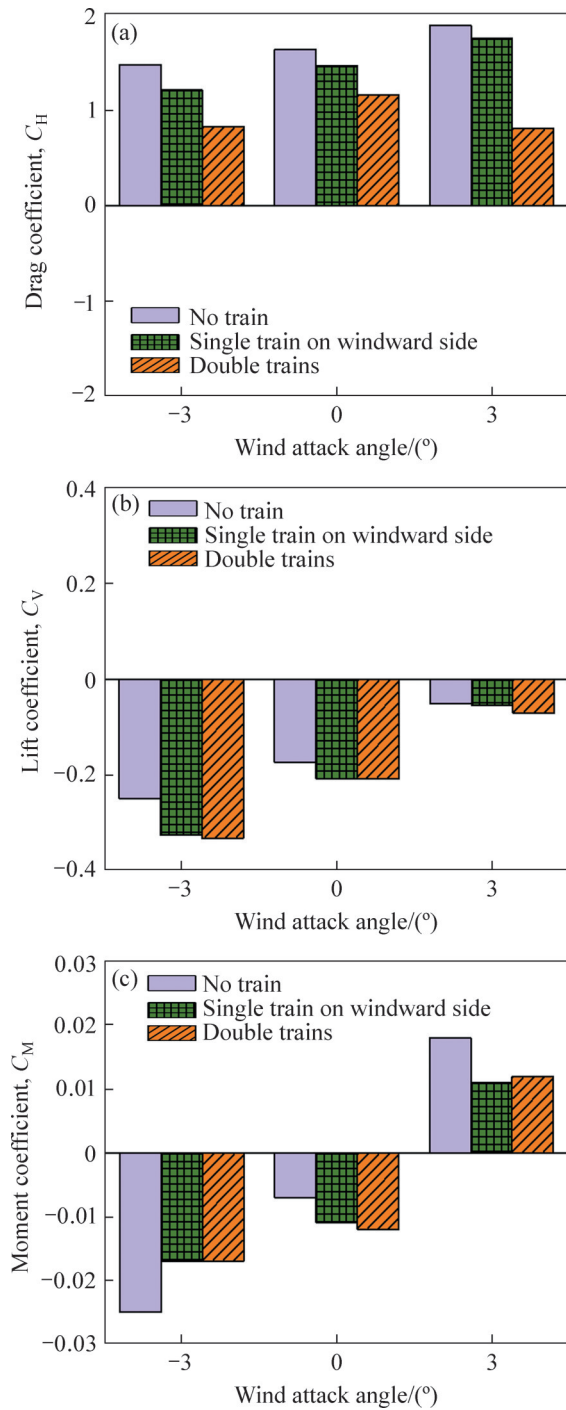
According to Tables 6 and 7, similar to the single train-girder system, the existence of double trains significantly reduces the drag coefficient of the girder, while the lift and moment coefficients change not obviously. For the train at windward side, both the drag and moment coefficients are very close between the single train case and the double trains case, and the lift coefficient of the single train case is smaller than that of the double trains case. Significantly, aerodynamic forces of the leeward train decrease sharply due to the shielding effect of the windward train, and then “recover” after the meeting. This severe fluctuating of the wind load acting on the leeward train could affect the stability of the train which is unfavorable to the comfort and safety of driving.

### 3.3.3 Comparison between different wind attack angles

Figure 7 shows the aerodynamic coefficients of girder at  $\alpha = -3^\circ, 0^\circ$  and  $3^\circ$  for different cases (namely without train, with single train and with double train). When a single train stays on the windward single of the girder, the drag coefficient of the girder decreases by 17.3%, 10.1% and 8% at  $\alpha = -3^\circ, 0^\circ$  and  $3^\circ$ , respectively, compared to the girder without a train. The drag coefficient of the girder decreases by 29.1%, 47.5% and 57.3%, respectively, at  $\alpha = -3^\circ, 0^\circ$  and  $3^\circ$  due to the existence of double trains compared to the girder without a train. Aerodynamic interference of the train reduces the moment coefficient of the girder at  $\alpha = -3^\circ$  and  $3^\circ$ , while it slightly increases the moment coefficient of the girder at  $\alpha=0^\circ$ .

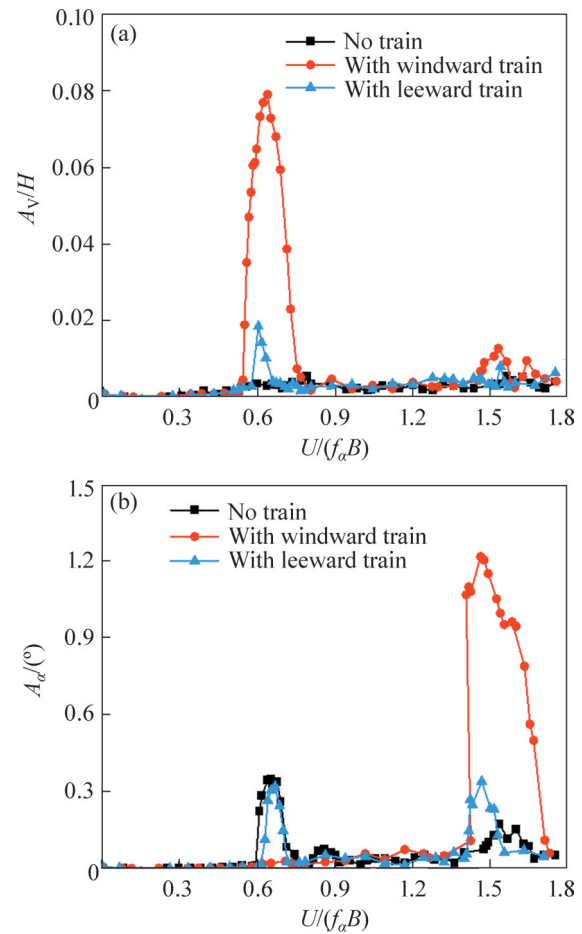
## 4 Results of vortex-induced vibration test

Figure 8 shows the variation of vibration amplitude with a reduced wind speed for the triple-box girder at  $\alpha=0^\circ$ . In Figure 8, the horizontal



**Figure 7** Influence of trains on aerodynamic coefficients of the girder at different wind attack angles: (a) Drag coefficient; (b) Lift coefficient; (c) Moment coefficient

coordinate is reduced wind speed  $U/(f_a B)$ , where  $f_a$  is the torsional vibration frequency of the model,  $A_v$  and  $A_a$  denote the vertical and torsional vibration amplitude of the girder respectively. Noteworthy, the existence of train will affect the frequency and equivalent quality of the girder. Therefore, the mass of train is considered for the sectional model in VIV



**Figure 8** VIV response of the girder (without aerodynamic measures, section II): (a) Vertical amplitude; (b) Torsional amplitude

test of the train-girder system. In other words, the increase of Scruton number caused by the train has been taken into account in the test. Besides, dimensionless wind speed  $U/(f_a B)$  is adopted in Figure 8, which can be converted into corresponding wind speed of full-scale bridge by employing the changed frequency of bridge girder caused by the train.

According to Figure 8, there is no obvious vertical VIV observed on the girder without a train (i.e., case B1). When a train is on the leeward side (case B3), the vertical VIV occurs in wind speed range of 0.57–0.65, and the maximum amplitude of  $A_v/H$  is close to 0.022. When a train is on the windward side (case B2), a strong vertical VIV occurs in the wind speed range 0.54–0.77 with a maximum amplitude of 0.079.

For the girder without a train (case B1), torsional VIV is observed in two wind speed ranges (i.e., 0.59–0.75 and 1.36–1.70), and the maximum

torsional amplitudes for the two VIV regions are  $0.351^\circ$  and  $0.174^\circ$ , respectively. When a single train is on the windward side of the girder (case B2), there is only one torsional VIV region, but the maximum torsional amplitude soars to  $1.22^\circ$ . When the train is on the leeward side (case B3), the maximum amplitude of the second torsional VIV region increases by two times compared with that of case B1, while there is no obvious change for the first VIV region.

To sum up, the existence of the train is unfavorable for the VIV performance of the triple-box girder, and the adverse effect of the train on the windward side is more significant than that on the leeward side.

## 5 Conclusions

Wind tunnel tests of aerodynamic force measurement and VIV test were carried out to investigate the aerodynamic interference effects between trains and the triple-box girder of bridges in this paper. Specifically, the interference effects on aerodynamic forces of the trains and girder, as well as VIV performance of the girder were involved. Conclusions are summarized as follows.

1) Aerodynamic interference effect between the triple-box girder and trains on static aerodynamic forces is remarkable, and the effect varies with the wind attack angle. When a single train stops on the girder, the horizontal position of the train has small effect on aerodynamic coefficients of the girder. When two trains meet on the girder, drag coefficient of the girder is significantly reduced compared with the conditions of no train or with a single train. existence of trains has a small impact on lift and moment coefficient of the girder.

2) Aerodynamic interference of the girder significantly reduces the drag coefficient of the train. When two trains meet on the girder, aerodynamic forces of the leeward train decrease first and then increases suddenly, and the severe fluctuation of aerodynamic force could cause remarkable train vibration, which is unfavorable to the driving safety and comfort.

3) A train stop on the triple-box girder could worsen the VIV performance of the girder. When the train is on the windward side, severe vertical and torsional VIV will occur on the girder. The adverse

effect of a windward side train is more significant than that of a leeward side train.

Existence of the train will change the flow field structure around the bridge, resulting in the change of surface pressure on the girder which could further lead to the variation of aerodynamic forces. However, the flow field structure is very complex due to the aerodynamic interference between the triple-box girder and auxiliary facilities, and it is difficult to explain the mechanism of aerodynamic interference effect based on existing test results. Visualization technology such as CFD or particle image velocimetry (PIV) could be a useful method to explore the specific mechanism of this phenomenon in the further study.

## Contributors

The overarching research goals were developed by HUA Xu-gang, WANG Chao-qun and CHEN Zheng-qing. YANG Ling-bo and WANG Chao-qun provided and analyzed the experimental data of wind tunnel test. HE Dong-sheng conducted the structure design of triple-box girder. The initial draft of the manuscript was written by YANG Ling-bo and WANG Chao-qun. All authors replied to reviewers' comments and revised the final version.

## Conflict of interest

YANG Ling-bo, HUA Xu-gang, WANG Chao-qun, HE Dong-sheng and CHEN Zheng-qing declare that they have no conflict of interest.

## References

- [1] HUANG Zhi-wen, LI Yan-zhe, HUA Xu-gang, et al. Automatic identification of bridge vortex-induced vibration using random decrement method [J]. *Applied Sciences*, 2019, 9(10): 2049. DOI: 10.3390/app9102049.
- [2] SARPKEYA T. A critical review of the intrinsic nature of vortex-induced vibrations [J]. *Journal of Fluids and Structures*, 2004, 19(4): 389–447. DOI: 10.1016/j.jfluidstructs.2004.02.005.
- [3] WANG Chao-qun, HUA Xu-gang, HUANG Zhi-wen, et al. Post-critical behavior of galloping for main cables of suspension bridges in construction phases [J]. *Journal of Fluids and Structures*, 2021, 101: 103205. DOI: 10.1016/j.jfluidstructs.2020.103205.
- [4] WANG Chao-qun, HUA Xu-gang, HUANG Zhi-wen, et al. Aerodynamic characteristics of coupled twin circular bridge hangers with near wake interference [J]. *Applied Sciences*, 2021, 11(9): 4189. DOI: 10.3390/app11094189.
- [5] HUA Xu-gang, WANG Chao-qun, LI Sheng-li, et al.



- Experimental investigation of wind-induced vibrations of main cables for suspension bridges in construction phases [J]. *Journal of Fluids and Structures*, 2020, 93: 102846. DOI: 10.1016/j.jfluidstructs.2019.102846.
- [6] XU Hai-jiang, DENG Hong-zhou, HU Xiao-yi, et al. Wind tunnel test on aerodynamic coefficients of multi-bundled conductors under skew winds [J]. *Journal of Fluids and Structures*, 2019, 91: 102702. DOI: 10.1016/j.jfluidstructs.2019.102702.
- [7] HU C, ZHOU Z, JIANG B. Effects of types of bridge decks on competitive relationships between aerostatic and flutter stability for a super long cable-stayed bridge [J]. *Wind and Structures*, 2019, 28(4): 255–270. DOI: 10.12989/was.2019.28.4.255.
- [8] LIU Jin-yang, HUI Yi, WANG Jing-xue, et al. LES study of windward-face-mounted-ribs' effects on flow fields and aerodynamic forces on a square cylinder [J]. *Building and Environment*, 2021, 200: 107950. DOI: 10.1016/j.buildenv.2021.107950.
- [9] HE Xu-hui, ZUO Tai-hui, ZOU Yun-feng, et al. Experimental study on aerodynamic characteristics of a high-speed train on viaducts in turbulent crosswinds [J]. *Journal of Central South University*, 2020, 27(8): 2465–2478. DOI: 10.1007/s11771-020-4462-3.
- [10] ZHU Si-yu, LI Yong-le, KOFFI T, et al. Case study of random vibration analysis of train-bridge systems subjected to wind loads [J]. *Wind & Structures*, 2018, 27(6): 399–416. DOI: 10.12989/was.2018.27.6.399.
- [11] WANG Bin, XU You-lin, ZHU Le-dong, et al. Determination of aerodynamic forces on stationary/moving vehicle-bridge deck system under crosswinds using computational fluid dynamics [J]. *Engineering Applications of Computational Fluid Mechanics*, 2013, 7(3): 355–368. DOI: 10.1080/19942060.2013.11015477.
- [12] HAN Yan, LIU Ye, HU Peng, et al. Effect of unsteady aerodynamic loads on driving safety and comfort of trains running on bridges [J]. *Advances in Structural Engineering*, 2020, 23(13): 2898–2910. DOI: 10.1177/1369433220924794.
- [13] BAKER C J, REYNOLDS S. Wind-induced accidents of road vehicles [J]. *Accident Analysis & Prevention*, 1992, 24(6): 559–575. DOI: 10.1016/0001-4575(92)90009-8.
- [14] SCHETZ J A. Aerodynamics of high-speed trains [J]. *Annual Review of Fluid Mechanics*, 2001, 33: 371 – 414. DOI: 10.1146/annurev.fluid.33.1.371.
- [15] LARSEN A, SAVAGE M, LAFRENIÈRE A, et al. Investigation of vortex response of a twin box bridge section at high and low Reynolds numbers [J]. *Journal of Wind Engineering and Industrial Aerodynamics*, 2008, 96(6–7): 934–944. DOI: 10.1016/j.jweia.2007.06.020.
- [16] NAGAO F, UTSUNOMIYA H, YOSHIOKA E, et al. Effects of handrails on separated shear flow and vortex-induced oscillation [J]. *Journal of Wind Engineering and Industrial Aerodynamics*, 1997, 69–71: 819–827. DOI: 10.1016/S0167-6105(97)00208-0.
- [17] KWOK K C S, QIN X R, FOK C H, et al. Wind-induced pressures around a sectional twin-deck bridge model: Effects of gap-width on the aerodynamic forces and vortex shedding mechanisms [J]. *Journal of Wind Engineering and Industrial Aerodynamics*, 2012, 110: 50 – 61. DOI: 10.1016/j.jweia.2012.07.010.
- [18] WU Bu-chen, LAIMA Shu-jin. Experimental study on characteristics of vortex-induced vibration of a twin-box girder and damping effects [J]. *Journal of Fluids and Structures*, 2021, 103: 103282. DOI: 10.1016/j.jfluidstructs.2021.103282.
- [19] DIANA G, RESTA F, ZASSO A, et al. Forced motion and free motion aeroelastic tests on a new concept dynamometric section model of the Messina suspension bridge [J]. *Journal of Wind Engineering and Industrial Aerodynamics*, 2004, 92(6): 441–462. DOI: 10.1016/j.jweia.2004.01.005.
- [20] DIANA G, RESTA F, BELLOLI M, et al. On the vortex shedding forcing on suspension bridge deck [J]. *Journal of Wind Engineering and Industrial Aerodynamics*, 2006, 94(5): 341–363. DOI: 10.1016/j.jweia.2006.01.017.
- [21] WANG Chao-qun, HUA Xu-gang, FENG Zhou-quan, et al. Experimental investigation on vortex-induced vibrations of a triple-box girder with web modification [J]. *Journal of Wind Engineering and Industrial Aerodynamics*, 2021, 218: 104783. DOI: 10.1016/j.jweia.2021.104783.
- [22] XU Liang, HUI Yi, YANG Qing-shan, et al. Modeling and modal analysis of suspension bridge based on continual formula method [J]. *Mechanical Systems and Signal Processing*, 2022, 162: 107855. DOI: 10.1016/j.ymsp.2021.107855.
- [23] HUA Xu-gang, WANG Chao-qun. Segment model wind tunnel test report on wind resistance research of Taoyamen bridge main bridge [R]. Key Laboratory for Wind and Bridge Engineering of Hunan Province, Hunan University, 2021. (in Chinese)
- [24] SIMIU E, SCANLAN R H. Wind effects on structures: an introduction to wind engineering [M]. Washington, D. C.: Wiley, 1978.
- [25] LI Yong-le, XU Xin-yu, GUO Jian-ming, et al. Wind tunnel tests on aerodynamic characteristics of vehicle-bridge system for six-track double-deck steel-truss railway bridge [J]. *Engineering Mechanics*, 2016, 33(4): 130 – 135. DOI: 10.6052/j.issn.1000-4750.2014.09.0741.
- [26] LI Tian, DAI Zhi-yuan, LIU Jia-li, et al. Review on aerodynamic drag reduction optimization of high-speed trains in china [J]. *Journal of Traffic and Transportation Engineering*, 2021, 21(1): 59 – 80. DOI: 10.19818/j.cnki.16711637.2021.01.003.

(Edited by HE Yun-bin)

## 中文导读

### 分离式三箱梁与列车间气动干扰效应对气动力系数及涡振性能的影响

**摘要：**为了研究列车与分离式三箱梁之间的气动干扰，进行了一系列风洞试验，重点研究了气动干扰对主梁和列车的三分力系数及主梁涡振性能的影响。采用列车和主梁的节段模型进行静力三分力测试和涡振试验。结果表明分离式三箱梁与列车之间存在显著的气动干扰效应。当单列车存在时，列车和主梁之间的相对水平位置对主梁的三分力系数影响不大。当双列车会车时，主梁的阻力系数较无列车和单列车时显著减小，且背风侧列车受到的气动力先突降后陡增，气动力的剧烈波动会引起列车的振动，对行车安全及舒适性不利。停靠在主梁上的列车对分离式三箱梁的涡振性能产生不利影响，会引起分离式三箱梁新的竖向涡振，且当列车位于迎风侧轨道上时，主梁扭转涡振振幅显著增加。

**关键词：**分离式三箱梁；风洞试验；车桥系统；气动干扰；涡激振动